Available online at www.sciencedirect.com
ScienceDirect
Trans. Nonferrous Met. Soc. China 28(2018) 2528−2537
Transactions of Nonferrous Metals Society of China
www.tnmsc.cn

Appropriate titanium slag composition during smelting of vanadium titanomagnetite metallized pellets

Shuai WANG, Yu-feng GUO, Tao JIANG, Feng CHEN, Fu-qiang ZHENG, Min-jun TANG, Ling-zhi YANG, Guan-zhou QIU

School of Minerals Processing and Bioengineering, Central South University, Changsha 410083, China

Received 15 November 2017; accepted 16 April 2018

Abstract: The suitable titanium slag composition with high titanium content for electric furnace smelting of vanadium titanomagnetite was investigated through thermodynamics and related phase diagram analysis. According to the thermodynamic results, low-melting-point regions and $MgTi_2O_5$ primary phase area in the phase diagrams, the suggested titanium slag composition for the present vanadium titanomagnetite metallized pellets should consist of 50% TiO_2, 8%−12% MgO and 13% Al_2O_3 (mass fraction) with a binary basicity of 0.8−1.2. Finally, the verified smelting experiments were conducted and successful separation of the molten iron from the titanium slag is obtained. The obtained vanadium-containing molten iron contains 0.681% V and 0.267% Ti, and the obtained titanium slag contains 52.21% TiO_2 (mass fraction), in which $MgTi_2O_5$ is the primary phase. The titanium resource in the final titanium slag production could be used to produce TiO_2 pigment by acid leaching methods.

Key words: vanadium titanomagnetite; electric furnace; basicity; MgO; $MgTi_2O_5$; titanium slag composition

1 Introduction

Titanium and vanadium are found in a large number of minerals, of which the vanadium titanomagnetite holds an important part. The Panxi region of Sichuan province in China possesses iron, vanadium and titanium resources. The proven deposits of titanium and vanadium account for 35.17% and 11.6% (mass fraction) of world total reserves, respectively [1]. The traditional blast furnace (BF) process has been utilized for these resources since the 1970s in China [2,3]. However, the traditional smelting technique causes serious problems such as poor permeability of the burden column, low smelting rates, high environmental pollution and high energy consumption [3,4]. In addition, the easily formed Ti(C,N) particles have high-melting-points and increase slag viscosity, then causing difficult separation of iron from titanium slag [5]. Ordinary iron ores have been mixed with the vanadium titanomagnetite concentrate to reduce the TiO_2 content of titanium slag for mitigation of titanium oxides reduction. As a result, the blast furnace titanium slag in $CaTiO_3$ primary phase field contains less than 25% (mass fraction) TiO_2, where the titanium resource cannot be recovered economically due to its low TiO_2 content. Therefore, many other methods [5−12] are developed to achieve the comprehensive utilization of vanadium titanomagnetite ore. The direct reduction−electric furnace (DR−EF) smelting process has been commercialized in South Africa and New Zealand, with mature production process, environment friendliness, a large scale of capacity and stable products quality [12]. Furthermore, compared to the BF process, the DR−EF process is proven beneficial for the accurate control of vanadium and titanium oxides reduction because the raw materials are heated by electrode [7]. However, reduction directions of vanadium and titanium oxides must be controlled for a successful separation between titanium slag and molten iron. In the Highveld Steel & Vanadium in South Africa, silica and dolomite have been added to dilute titania and mitigate the titanium oxides reduction [13,14]. As a result, the produced titanium slag contains less than 35% (mass fraction) TiO_2 but without effectively recovering method due to its low TiO_2 content.

One of the keys to utilize the vanadium titanomagnetite by the DR−EF process is to suppress the reduction of titanium oxides. In addition, a higher

Corresponding author: Yu-feng GUO, Tel: +86-731-88830542, E-mail: yfguo@csu.edu.cn; Tao JIANG, Tel: +86-731-88710804, E-mail: jiangtao@csu.edu.cn
DOI: 10.1016/S1003-6326(18)64899-X

TiO_2-content slag should be obtained to increase the titanium recovery ratio. Previous research [7,15] indicated that titanium resource was easier and more economical to be recovered by acid leaching method if the electric furnace titanium slag had higher content of TiO_2. The primary phase of commercially produced titanium slags is $CaTiO_3$, and thus, it is difficult to recover titanium from the titanium slags due to the poor acid solubility of $CaTiO_3$. Therefore, the titanium slag composition, which is beneficial for electric smelting, along with a higher TiO_2 content, should be found. BOROWIEC and ROSENQVIST [16] showed that MgO addition could stabilize the M_3O_5 phase (M_3O_5, M=Fe, Mg) in the Fe−Ti−Mg−O system. It can be inferred that the amount of carbon addition and the quantity of the additives should be accurately controlled in order for a high TiO_2 titanium slag to be obtained. In addition, TANG et al [17] showed that the successful melting separation of high-chromium vanadium-bearing titanomagnetite metallized pellet was achieved with melting temperature of 1625 °C, melting time of 40−50 min, 2% (mass fraction) CaF_2 and basicity of 1.1. LV et al [18] showed that the effective separation of iron and titanium slag could be realized by melting metallized pellets at 1550 °C for 60 min with the addition of 1% (mass fraction) CaO (basicity of 1.1) and 2% (mass fraction) graphite powder. Also, the effects of slag composition on the reduction behaviors of iron, vanadium and titanium oxides were reported in our previous papers [19,20]. Briefly, even though many previous works [21−25] about the blast furnace titanium slag were done, the suitable composition of higher titanium slag with $MgTi_2O_5$ as the main phase for smelting vanadium titanomagnetite by the DR−EF process is not very clear.

In this work, the thermodynamics and the related phase diagrams are investigated to obtain the suitable titanium slag compositions that can mitigate the titanium reduction and produce a higher titanium slag. Finally, the high-temperature smelting experiments are carried out. Our findings will provide a technical basis for successful smelting of vanadium titanomagnetite by the DR−EF process.

2 Experimental

2.1 Materials

The vanadium titanomagnetite concentrate was obtained from the Panxi region of China, whose total iron grade was as high as 54.97% with 12.22% TiO_2 and 0.65% V_2O_5 (mass fraction). Figure 1 shows the whole flow-chart of the process. As shown in Fig. 1, the vanadium titanomagnetite concentrate pellets were reduced by coal in a rotary kiln (diameter: 1000 mm, and length: 550 mm, produced in Central South University, China) at 1100 °C with a C/Fe mass ratio of 1:1. The chemical composition of the metallized pellet is listed in Table 1. The analytically pure graphite powder was used as the reductant. All reagents used in this study were of analytical grade. The basicity in this work was defined as a CaO to SiO_2 mass ratio.

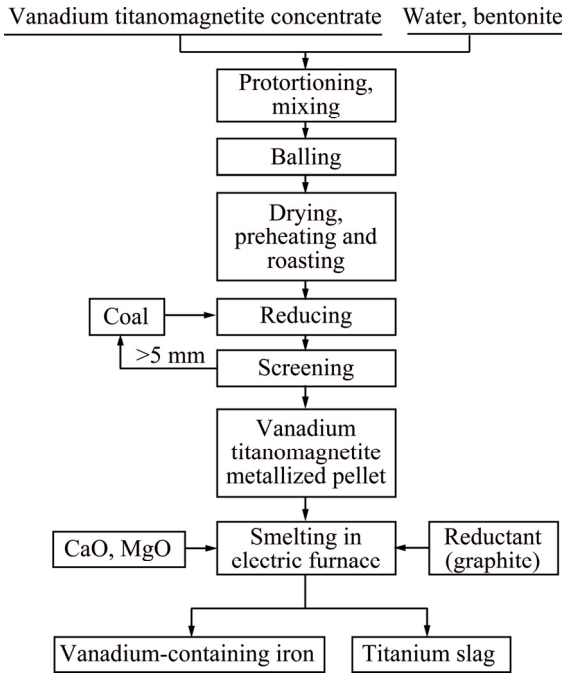

Fig. 1 Flow sheet of present direct reduction−electric furnace (DR−EF) process

Table 1 Chemical composition of metallized pellet (mass fraction, %) [19]

TFe*	MFe*	TiO_2	V_2O_5	CaO
71.38	64.56	15.53	0.82	1.01
SiO_2	MgO	Al_2O_3	C	S
3.71	2.58	3.83	0.036	0.027

*—Total Fe; **—Metallic Fe

The phase composition of the metallized pellet sample was characterized by an X-ray diffractometer and the major phases were metallized iron (α-Fe), ferrous−pseudobrookite ($Fe_{1-x}Mg_xTi_2O_5$, $0\leq x\leq 1$) and magnesia−alumina spinel [19].

2.2 Thermodynamic analysis method

In order to investigate the reduction process of complicated titanium oxides in metallized pellet during DR−EF process, the smelting equilibrium results were carried out by FactSage 7.0 [26]. In addition, The $CaO-SiO_2-MgO-TiO_2-Al_2O_3$ phase diagrams were drawn by FactSage 7.0 to find the suitable titanium slag compositions. Modules were “Phase Diagram” and “Equilib” with databases “FToxid” and “FactPS”.

2.3 Experimental apparatus

2.3.1 Electric furnace experiment

The high-temperature smelting experiments were conducted in a $MoSi_2$ furnace, as shown in our previous work [19]. First, the crushed metallized pellets (<1 mm) were mixed with the required amount of additives (CaO, MgO and graphite powder), and then the mixture was placed in a graphite crucible (diameter: 50 mm, and height: 100 mm). Afterwards, the graphite crucible with the mixture was placed in the electric furnace and heated to 1550 °C. High pure argon (>99.999%) was used as the protective gas during the smelting process. Finally, after the smelting duration was up, the crucible was quickly taken out and cooled with the protection of high pure argon. The iron and slag samples were separated for following analysis.

2.3.2 Induction furnace experiment

As shown in Fig. 2, a smelting experiment of vanadium titanomagnetite was also carried out in an induction furnace of 50 kW. The experimental smelting temperature was represented by the surface temperature of slag, and the surface temperature was measured with the infrared temperature measurement system. Moreover, the metallized pellets (4 kg) were mixed with flux (108 g CaO and 18 g MgO) and graphite powder (150 g), and then the mixtures were placed into a graphite crucible (diameter: 200 mm, and height: 300 mm), which was located in the center of the furnace. Next, the graphite crucible was sealed using the matching graphite cap, and the electric power was turned on to start heating and smelting. During the smelting process, the experimental phenomenon was observed and the smelting temperature was measured. Furthermore, the bubbles in the slag were quickly observed through opening the cap and the bubbles formation was used to judge the chemical reactions. After the temperature was increased to 1600 °C and no bubbles in slag were observed, smelting temperature was kept for 10 min, then the power was cut off and the samples were cooled naturally.

The solidified samples were removed from the crucible, the chemical composition of the titanium slag was analyzed by X-ray fluorescence (XRF) (PANalytical Axios mAX, PANalytical B.V., Almelo, Netherlands) and the chemical composition of the iron was analyzed by chemical analysis methods. The major phases of the titanium slag were determined by X-ray Diffraction (XRD) (Cu K_α radiation, λ=1.54056 Å, D/Max2200, Rigaku, Japan). In addition, the microstructure of the titanium slag was analyzed with optical microscope (Lecia, DM4500P, Germany).

3 Results and discussion

3.1 Thermodynamic analysis

Theoretically, according to the chemical composition and the major phases of the vanadium titanomagnetite metallized pellet, the probably existed compounds containing iron and titanium are $FeTi_2O_5$, $MgTi_2O_5$, TiO_2, Ti_3O_5 and Al_2TiO_5. Furthermore, $CaTiO_3$ and $CaSiTiO_5$ are probably formed when the slag composition is adjusted by adding CaO and MgO. In addition, according to the results of our previous investigations [19,20], the suitable target minerals in the titanium slag should be $MgTi_2O_5$, $MgTiO_3$, $CaTiO_3$, $CaSiTiO_5$ and Al_2TiO_5 because they have higher starting reduction temperatures when they are reduced to TiO and TiC.

However, it is generally accepted that the titanium slag with a higher TiO_2 content is beneficial to be utilized to recover the titanium resource by leaching methods. Thus, it is clear that $CaSiTiO_5$ and Al_2TiO_5 are inappropriate as the target minerals due to their low titanium contents. Therefore, $MgTi_2O_5$, $MgTiO_3$ and $CaTiO_3$ are the suitable minerals in titanium slag. What is more, in consideration of the following utilization of titanium slag, the $MgTi_2O_5$ and $MgTiO_3$ are more suitable as the major mineral phases of titanium slag because titanium resource in $CaTiO_3$ is not suitable to be recovered by acid leaching methods due to its poor acid solubility. Thus, $MgTi_2O_5$ and $MgTiO_3$ are chosen as the primary phases of the electric furnace titanium slag.

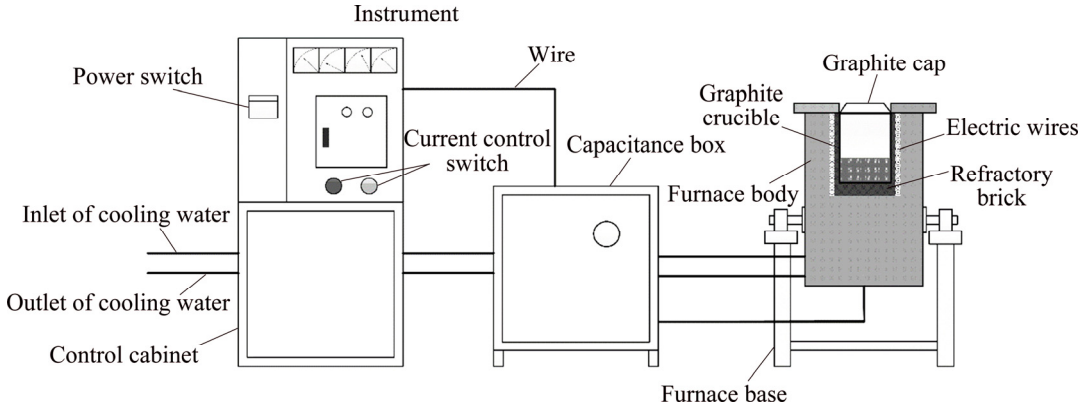

Fig. 2 Schematic diagram of medium-frequency induction furnace

3.2 Phase diagram analysis

Generally, uniform and flowing liquid slag is beneficial for successful smelting. Besides, smelting temperature should be higher than melting point of slag to obtain slag with suitable physical and chemical properties [27]. Especially, a low melting temperature of slag is required to satisfy smooth smelting operation and reduce energy consumption.

The melting point and primary phase of titanium slag can be determined from the phase diagram with solidus projections. Therefore, in order to find the suitable composition of electric furnace titanium slag with high TiO_2 content, the TiO_2−CaO−SiO_2−MgO−Al_2O_3 phase diagrams were analyzed using FactSage 7.0. According to the thermodynamic analysis, MgO and CaO were added during smelting process, whereas the contents of SiO_2 and Al_2O_3 were kept constant. Furthermore, according to the present chemical composition of metallized pellet (Table 1), it is calculated that when the TiO_2 content is increased to about 50% (mass fraction), the SiO_2 content is almost 11%, whereas the Al_2O_3 content is almost 13% and MgO content is approximately 8% (mass fraction).

Figure 3 shows the TiO_2−SiO_2−CaO−MgO−Al_2O_3 system with solidus projection (w(MgO)=8% and w(Al_2O_3)=13%). It can be seen that with the increase of CaO content, the solid silica−calcium compounds are generated, where the $CaTiO_3$ forms with the high TiO_2 content. However, the $CaTiO_3$ has a high melting temperature and the melting point of the slag will increase as the $CaTiO_3$ content increases in the slag. It is indicated that the binary basicity should be controlled at about 1.0 because the high basicity promotes $CaTiO_3$ formation.

The phase diagram with solidus projection of TiO_2−MgO−CaO−SiO_2−Al_2O_3 (w(SiO_2)=11%, and w(Al_2O_3)=13%) is shown in Fig. 4. Figure 4 indicates that the amount of $CaTiO_3$ increases and the liquid region decreases with the increase of CaO content, while the liquid region expands as the MgO content increases. Moreover, increasing the MgO content can promote the generation of magnesia−titania compounds, as well as increase the content of the pseudobrookite in the titanium slag.

It is shown that the low melting point region is almost located in the central part of the phase diagram, while the overmuch CaO and MgO increase the liquidus temperatures. This means that both CaO and MgO should be controlled with suitable ranges.

Moreover, through the analysis of thermodynamic and phase diagrams, the suitable compositions of titanium slag are summarized as follows: about 50% TiO_2, 11% SiO_2, and 13% Al_2O_3 (mass fraction), while the binary basicity is 0.8−1.2 and the content of MgO ranges from 8% to 12% (mass fraction).

Figure 5 illustrates the CaO−SiO_2−MgO−Al_2O_3−TiO_2 phase diagram (w(TiO_2)=50% and w(Al_2O_3)=13%).

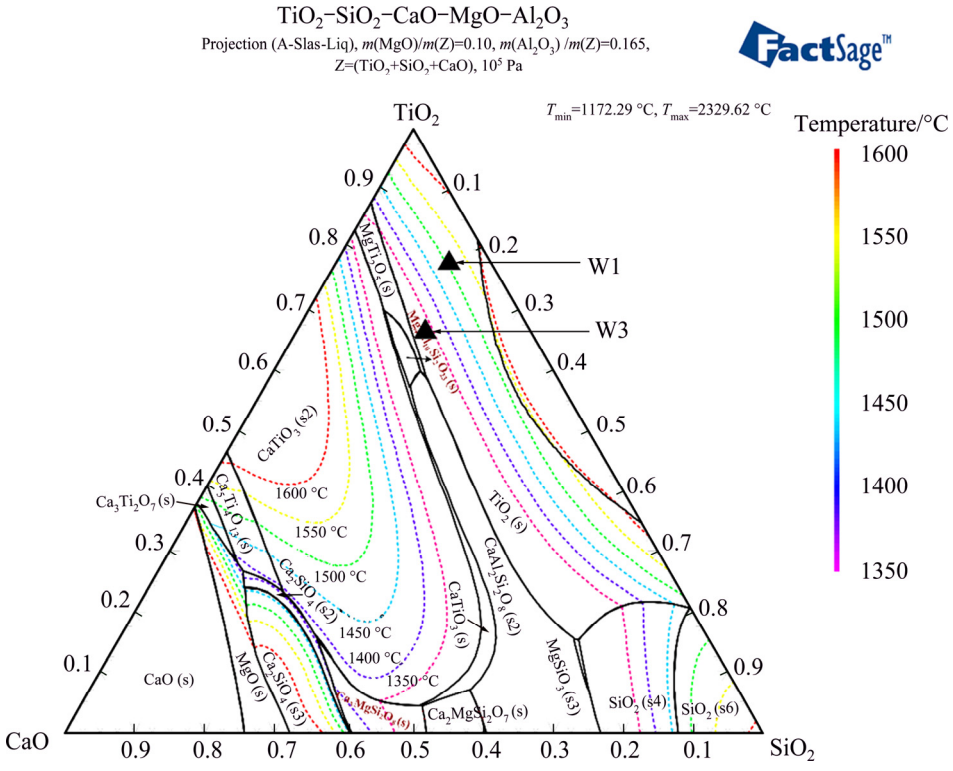

Fig. 3 Phase diagram of TiO_2−SiO_2−CaO−MgO−Al_2O_3 (w(MgO)=8% and w(Al_2O_3)=13%)

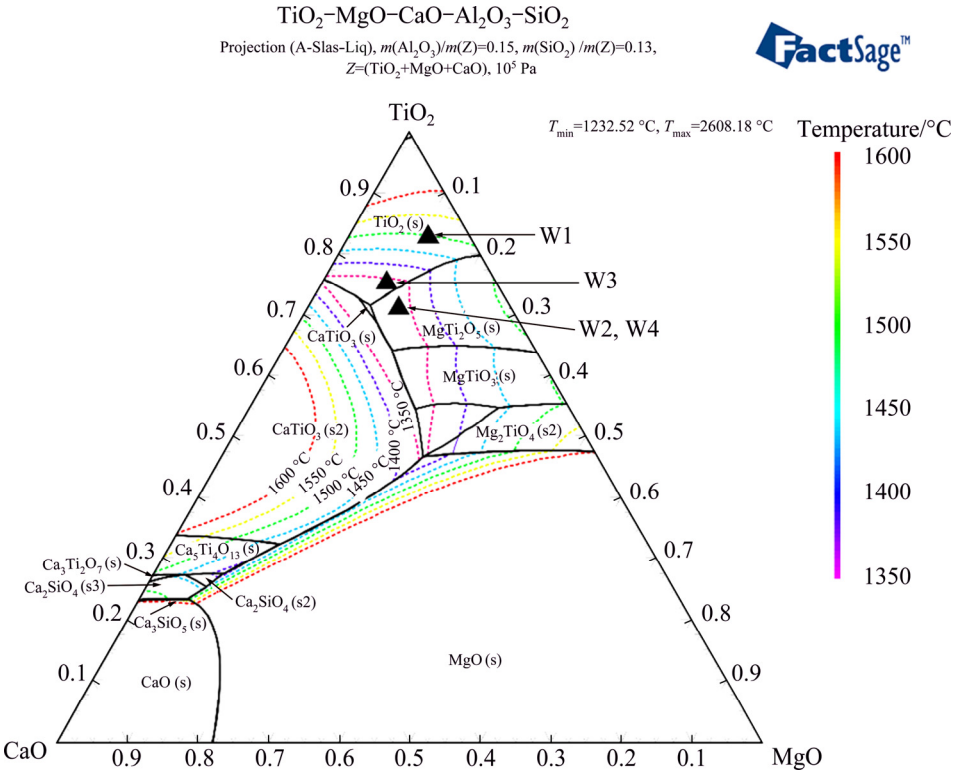

Fig. 4 Phase diagram of TiO_2−MgO−CaO−SiO_2−Al_2O_3 ($w(SiO_2)$=11% and $w(Al_2O_3)$=13%)

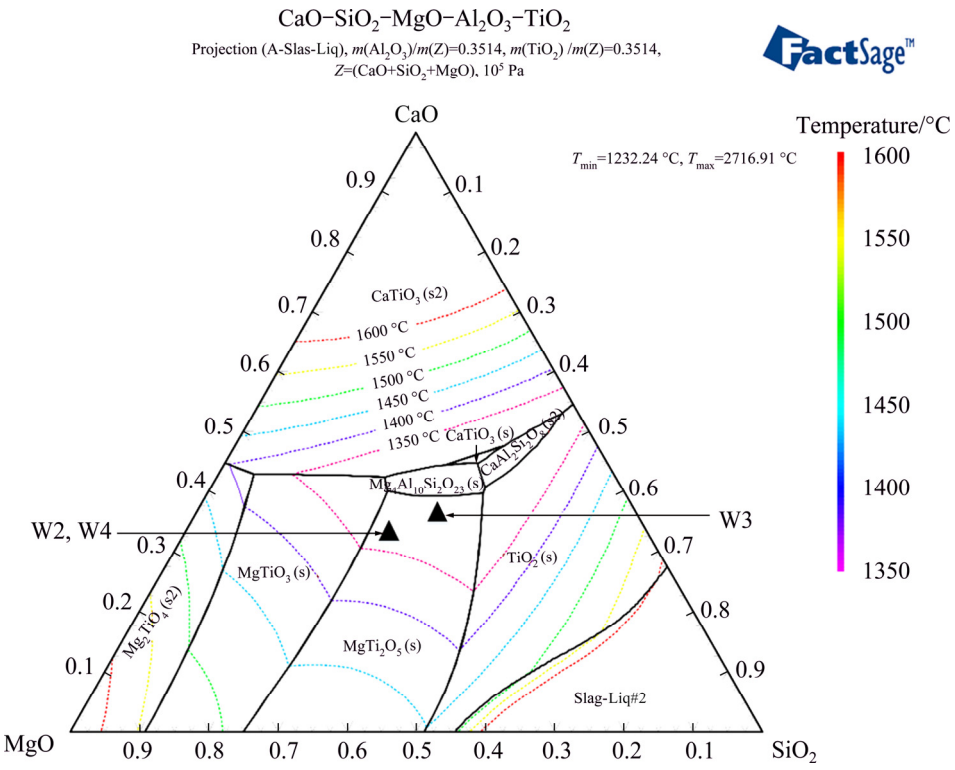

Fig. 5 Phase diagram of CaO−SiO_2−MgO−Al_2O_3−TiO_2 ($w(TiO_2)$=50% and $w(Al_2O_3)$=13%)

3.3 Equilibrium calculation in smelting process

It is well known that the Ti content in the molten iron increases when the titanium oxides are excessively reduced during the smelting process. Therefore, it is reasonable to use the Ti, V and Si contents in the molten iron to evaluate the reduction situations of the titanium, vanadium and silicon oxides. In addition, a fine balance between low enough titanium levels in the iron (as a

proxy for maintaining the right temperature), and high enough titanium reduction (indicative of conditions which are sufficiently strongly reducing) is maintained. This balance seems to be between 0.15% and 0.20% (mass fraction) titanium [12]. Above 0.2% Ti, an over-reduced condition is seen, while the highly reducing conditions, leading to the formation of solid TiC or TiO−TiC solid solutions, cause the apparent viscosity to increase [12]. Therefore, the contents of Ti, Si and V in the molten iron were calculated using FactSage software. The effects of binary basicity, MgO content and carbon addition on the Ti, Si and V contents in the molten iron are shown in Figs. 6, 7 and 8, respectively.

As shown in Fig. 6, the contents of Ti and Si in the molten iron decrease as the slag basicity increases, whereas the V content shows an unobvious change.

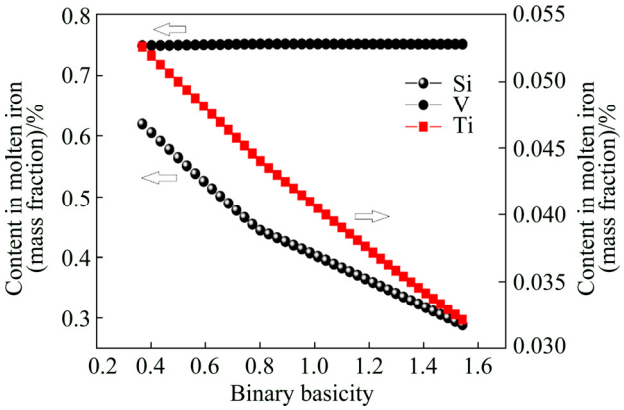

Fig. 6 Effect of binary basicity on Ti, Si and V contents in molten iron

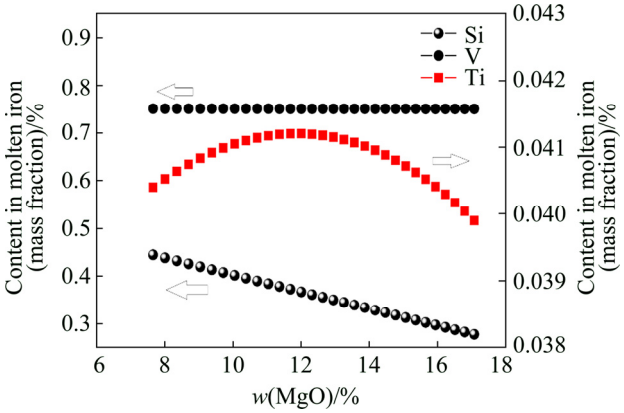

Fig. 7 Effects of MgO content on Ti, Si and V contents in molten iron

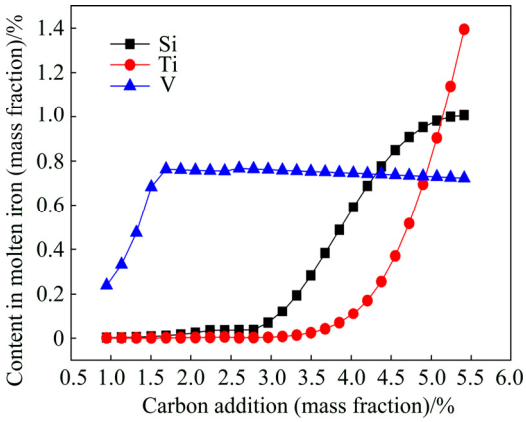

Fig. 8 Effects of carbon addition on Ti, Si and V contents in molten iron

In addition, Fig. 7 illustrates that the Ti content in the molten iron increases firstly and then decreases while the Si content in the iron gradually decreases with the increase of MgO content in slag. However, the V and Ti contents in the iron have imperceptive changes with the increase of MgO content.

Figure 8 shows the effects of carbon addition on the contents of Ti, V and Si in the iron. It can be seen that the V content dramatically increases as the carbon addition increases from 0.5% to 1.6% (mass fraction), but changes imperceptibly as carbon addition is above 1.6%. Furthermore, the Ti and Si contents are at low levels as the carbon addition is below 3%, then they sharply increase as the carbon addition beyond 3% (mass fraction). Thus, the quantity of carbon addition should be controlled accurately from about 1.6% to almost 4.2% (mass fraction).

3.4 Experiments in high temperature electric furnace

In this work, the smelting experiments were conducted in a high-temperature electric furnace to verify the analysis results of the thermodynamics and the phase diagrams. The designs of experiments and smelting parameters are listed in Table 2. The chemical composition locations of experiments slag are illustrated in the phase diagrams (seen in Figs. 3, 4, and 5).

As given in Table 3, the V content in the iron increases as the basicity increases, which means that the vanadium oxides reduction is improved as the basicity increases. The higher vanadium content in the iron is

Table 2 Smelting parameters of smelting experiments

No.	Binary basicity	*w*(MgO)/%	Smelting temperature/°C	Smelting duration/min	*w*(reductant)/%
W1	0.3	8.23	1550	20	2
W2	1.0	11.43	1550	20	2
W3	1.0	8.34	1550	20	3
W4	1.0	11.38	1550	20	5

beneficial to the vanadium extraction in the following converter furnace process. Furthermore, the Ti and Si contents in the iron decrease as the basicity increases, which indicates that increasing basicity can mitigate the reductions of titanium and silicide oxides. In addition, Figs. 3, 4 and 5 show that the increase of the basicity promotes the generation of $CaTiO_3$ phase and the addition of MgO is beneficial to $MgTi_2O_5$ formation. The formation of TiC is suppressed with the increase of amounts of $CaTiO_3$ and $MgTi_2O_5$ phases in the slag [20]. Table 3 also indicates that the target of smelting vanadium titanomagnetite is achieved through adjusting the titanium slag compositions according to the analysis results.

In addition, the present results were compared with the previous investigations to discuss the general application of the present investigation results with the variation of vanadium titanomagnetite ores. Table 4 gives the chemical composition and smelting parameters of previous investigations. It is clear that the used vanadium titanomagnetite ore had different chemical compositions. Table 5 gives the chemical and phase compositions of the titanium slags in previous investigations [17,18,28]. It can be seen that the titanium slag obtained by LV et al [18] has a similar composition with the present titanium slag. However, the TiO_2 content of vanadium titanomagnetite metallized pellets in TANG et al [17] and LI et al [28] is lower than that in the present material, and as a result, they produced the titanium slag with a lower TiO_2 contents. Furthermore, the phase compositions of the titanium slags obtained by different researchers are similar, and the main phase is $MgTi_2O_5$. Briefly, the present results can also be used to guide the smelting of vanadium titanomagnetite ore which has a similar chemical composition with the present ore.

3.5 Experiments in medium-frequency induction heating furnace

According to the thermodynamics and phase diagrams analysis, the verified experiment was carried out. The metallized pellets (4 kg) were mixed with graphite powder (150 g), and then smelted in a medium-frequency induction heating furnace under the conditions of binary basicity (CaO/SiO_2) of 1.18, smelting temperature of 1600 °C for 10 min, and the content of MgO of about 11% (mass fraction). The chemical compositions of vanadium-containing iron are given in Table 6. Table 7 shows the main chemical compositions of vanadium-containing irons produced in different countries with different processes.

Table 6 shows that the vanadium-containing molten iron contains 0.681% V, 0.267% Ti and 0.185% Si (mass

Table 3 Chemical compositions of titanium slag and vanadium-bearing iron

No.	Titanium slag						Vanadium-bearing iron			
	$w(TiO_2)$/%	w(CaO)/%	$w(SiO_2)$/%	w(MgO)/%	$w(Al_2O_3)$/%	Basicity	w(Fe)/%	w(V)/%	w(Ti)/%	w(Si)/%
W1	52.36	3.98	11.04	8.29	12.88	0.36	97.26	0.096	0.482	0.333
W2	47.87	11.57	11.43	11.43	10.69	1.01	98.12	0.564	0.372	0.208
W3	52.12	12.57	11.75	8.34	13.93	1.07	98.94	0.597	0.126	0.128
W4	50.34	11.79	11.68	11.38	13.05	1.01	98.09	0.683	0.296	0.199

Table 4 Comparison of chemical composition of metallized pellet and smelting parameter from different references

Source	Chemical composition (mass fraction)/%					Smelting parameter	
	TiO_2	CaO	SiO_2	MgO	Al_2O_3	Temperature /°C	Time/min
Present study	15.53	1.01	3.71	2.58	3.83	1550	20
TANG et al [17]	8.19	0.34	3.16	1.55	4.25	1625	40−50
LV et al [18]	15.82	0.48	1.35	2.16	4.11	1550	60
LI et al [28]	9.11	0.73	4.20	2.43	2.38	1600	50

Table 5 Comparison of chemical and phases compositions of slags from different references

Source	Chemical composition (mass fraction)/%					Slag basicity	Phase composition
	TiO_2	CaO	SiO_2	MgO	Al_2O_3		
Present study	50.34	11.79	11.68	11.38	13.05	1.01	$MgTi_2O_5$, $CaTiO_3$, $Mg_3Al_2CaSi_2O_6$
TANG et al [17]	37.52	–	–	–	–	1.1	$MgTi_2O_5$, $CaTiO_3$, Fe_2TiO_5, $Ca_3Al_2O_6$
LV et al [18]	54.87	8.01	7.26	9.21	13.85	1.1	$MgTi_2O_5$, $MgAl_2O_4$, $CaSiO_3$
LI et al [28]	40.63	15.92	20.75	11.22	10.42	0.77	$MgTi_2O_5$, $CaTiO_3$, $CaMgSi_2O_6$, $Ca_3Al_2O_6$

Table 6 Chemical composition of vanadium-bearing iron (mass fraction, %)

Total Fe	V	Ti	Si	Mg	Al	Ca	S	P
97.45	0.681	0.267	0.185	0.01	0.004	0.001	0.05	0.02

Table 7 Comparison of chemical compositions of vanadium-bearing iron with different processes (mass fraction, %) [29]

Location	V	Si	Ti	S	P	Process
NTMK(Russia)	0.43	0.46	0.30	0.044	0.060	BF−BOF
PZHIS* (China)	0.33	0.25	0.25	0.072	0.031	BF−BOF
South Africa	1.28	0.25	0.16	0.065	0.075	DR−EF**
New Zealand	0.45	0.11	0.16	0.060	0.060	DR−EF
Present work	0.681	0.185	0.267	0.05	0.02	DR−EF

*PZHIS represents Panzhihua Iron and Steel Group in China. **DR−EF represents direct reduction−electric furnace process

fraction). Compared to the compositions of the vanadium-containing iron produced by BF process in Table 7, it is clear that the quality of product produced by the DR−EF process is better than that of the production from the blast furnace process. As shown in Table 7, the main chemical compositions of vanadium-containing iron are not much different from other molten irons. It could be inferred that the properties of the vanadium-containing molten iron in this study have little difference with other vanadium-containing irons produced by other processes. The vanadium-containing molten iron in this study satisfies the requirement for the subsequent steelmaking and production of vanadium slag. Table 7 shows that the Ti content in the present experiment is close to that in the iron produced by the blast furnace process in PZHIS (China) and lower than that in the iron produced in NTMK (Russia). As the Ti content in molten iron represents the titanium oxides reduction, by considering the successful blast furnace smelting in Russia and China, it is also indicated that the titanium oxides reduction in the present study are also successfully controlled to suppress the titanium carbide formation.

Table 8 shows that the TiO_2 content of the titanium slag is 52.21% (mass fraction), which is higher than the grade of TiO_2 in titanium concentrate (~47%, mass fraction), and the titanium slag satisfies the requirement for the following titanium extraction by sulfuric acid leaching process. Besides, Fig. 9 shows the XRD patterns of the titanium slag. The major phases of titanium slag are pseudobrookite ($MgTi_2O_5$), with minor perovskite ($CaTiO_3$) and magnesium aluminum silicate phases. The microstructural image is displayed in Fig. 10. It can be seen that the perovskite and pseudobrookite are distributed in the titanium slag. Furthermore, it is well known that the titanium carbide is dispersed in the titanium slag with quite fine size. Generally, the perovskite phase crystals are fine dispersing floc, spicule or cruciate, and then the small crystals grow into column crystals [30]. As illustrated in Fig. 10, the titanium carbide is not observed in the microstructural image of the titanium slag. In addition, the XRD analysis also indicates that the primary phase is $MgTi_2O_5$ and the generation of titanium carbide does not occur. It can be explained that the titanium oxides reduction is mitigated under this smelting conditions. Figure 11 illustrates that

Table 8 Chemical composition of titanium slag (mass fraction, %)

TiO_2	CaO	SiO_2	MgO	Al_2O_3	TFe	V_2O_5	MnO
52.21	13.56	12.01	11.05	13.10	0.999	0.118	0.56

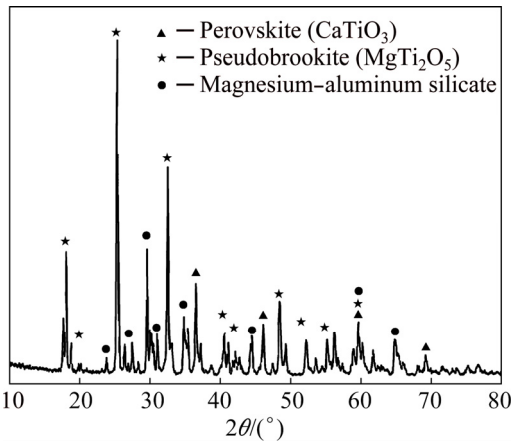

Fig. 9 XRD pattern of titanium slag

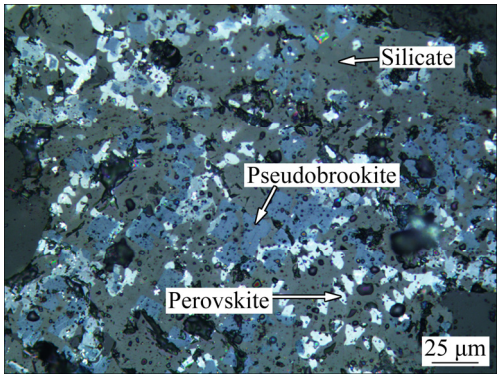

Fig. 10 Microstructural image of titanium slag

Fig. 11 Macro picture of vanadium-containing iron and titanium slag

successful separation between the titanium slag and the molten iron is obtained.

4 Conclusions

1) The suitable composition of titanium slag for the direct reduction−electric furnace process was analyzed through the related thermodynamics and the phase diagrams which were calculated using FactSage 7.0. The verified experiments were carried out in a high-temperature electric furnace and an induction furnace.

2) The analysis of thermodynamics and phase diagrams indicates that the suitable complicated titanium oxides are $MgTi_2O_5$ and $MgTiO_3$. According to the low-melting-point regions and the $MgTi_2O_5$ phase area in the phase diagrams, the suitable titanium slag compositions are about 50% TiO_2, 12% SiO_2 and 13% Al_2O_3 (mass fraction), while the range of binary basicity is 0.8−1.2 and the content of MgO ranges from 8% to 12% (mass fraction).

3) The experiments in induction furnace were carried out and the results show that the high-titanium slag with $MgTi_2O_5$ as primary phase containing 52.21% (mass fraction) TiO_2 and the vanadium-bearing iron containing 0.681% (mass fraction) V are obtained at 1600 °C for 10 min with basicity of 1.18 and 11% (mass fraction) MgO.

References

[1] TAYLOR P R, SHUEY S A, VIDAL E E, GOMEZ J C. Extractive metallurgy of vanadium containing titaniferous magnetite ores: A review [J]. Minerals and Metallurgical Processing, 2006, 23: 80−86.

[2] GUO Pei-min, ZHAO Pei. Technical analysis on selective separation and enrichment of Ti-bearing blast furnace slag based on phase diagrams [J]. Iron Steel Vanadium Titanium, 2005, 26: 5−10. (in Chinese)

[3] FU Wei-guo, WEN Yong-cai, XIE Hong-en. Development of intensified technologies of vanadium-bearing titanomagnetite smelting [J]. Journal of Iron and Steel Research, International, 2011, 18: 7−10.

[4] LIU Shui-shi, GUO Yu-feng, QIU Guan-zhou, JIANG Tao. Solid-state reduction kinetics and mechanism of pre-oxidized vanadium–titanium magnetite concentrate [J]. Transactions of Nonferrous Metals Society of China, 2014, 24: 3372−3377.

[5] LV Xue-wei, LUN Zhi-gang, YIN Jia-qing, BAI Chen-guang. Carbothermic reduction of vanadium titanomagnetite by microwave irradiation and smelting behavior [J]. ISIJ International, 2013, 53: 1115−1119.

[6] ZHAO Long-sheng, WANG Li-na, CHEN De-sheng, ZHAO Hong-xin, LIU Ya-hui, QI Tao. Behaviors of vanadium and chromium in coal-based direct reduction of high-chromium vanadium-bearing titanomagnetite concentrates followed by magnetic separation [J]. Transactions of Nonferrous Metals Society of China, 2015, 25: 1325−1333.

[7] ZHENG Fu-qiang, CHEN Feng, GUO Yu-feng, JIANG Tao, TRAVYANOV A Y, QIU Guan-zhou. Kinetics of hydrochloric acid leaching of titanium from titanium-bearing electric furnace slag [J]. JOM, 2016, 68: 1476−1484.

[8] JENA B C, DRESLER W, REILLY I G. Extraction of titanium, vanadium and iron from titanomagnetite deposits at pipestone lake, Manitoba, Canada [J]. Minerals Engineering, 1995, 8: 159−168.

[9] WANG Zhen-yang, ZHANG Jian-liang, XING Xiang-dong, LIU Zheng-jian. Congregated electron phase and Wagner model applied in titanium distribution behavior in low-titanium slag [J]. Transactions of Nonferrous Metals Society of China, 2015, 25: 1640−1647.

[10] LU Chang-yuan, ZOU Xing-li, LU Xiong-gang, XIE Xue-liang, ZHENG Kai, XIAO Wei, CHENG Hong-wei, LI Guang-shi. Reductive kinetics of Panzhihua ilmenite with hydrogen [J]. Transactions of Nonferrous Metals Society of China, 2016, 26: 3266−3273.

[11] GOU Hai-peng, ZHANG Guo-hua, HU Xiao-jun, CHOU Kuo-chi. Kinetic study on carbothermic reduction of ilmenite with activated carbon [J]. Transactions of Nonferrous Metals Society of China, 2017, 27: 1856−1861.

[12] STEINBERG W S. Development of a control strategy for the open slag bath furnaces at Highveld Steel and Vanadium Corporation Ltd [D]. University of Pretoria, 2008.

[13] NAFZIGER R H, JORDAN R R. Prereduction and melting of domestic titaniferous materials [J]. Metallurgical and Materials Transactions B, 1983, 14: 55−62.

[14] STEINBERG W S, GEYSER W, NELL J. The history and development of the pyrometallurgical processes at Evraz Highveld Steel & Vanadium [J]. Journal of the Southern African Institute of Mining and Metallurgy, 2011, 111: 705−710.

[15] ZHENG Fu-qiang, GUO Yu-feng, LIU Shui-shi, QIU Guan-zhou, CHEN Feng, JIANG Tao, WANG Shuai. Removal of magnesium and calcium from electric furnace titanium slag by H_3PO_4 oxidation roasting–leaching process [J]. Transactions of Nonferrous Metals Society of China, 2018, 28: 356−366.

[16] BOROWIEC K, ROSENQVIST T. Phase relations and oxygen potentials in the Fe−Ti−Mg−O system [J]. Scandinavian Journal of Metallurgy, 1985, 14: 33−43.

[17] TANG Jue, CHU Man-sheng, FENG Cong, TANG Ya-ting, LIU Zheng-gen. Melting separation behavior and mechanism of high-chromium vanadium–bearing titanomagnetite metallized pellet got from gas-based direct reduction [J]. ISIJ International, 2016, 56: 210−219.

[18] LV Chao, YANG Kun, WEN Shu-ming, BAI Shao-jun, FENG Qi-cheng. A new technique for preparation of high-grade titanium slag from titanomagnetite concentrate by reduction−melting−magnetic separation processing [J]. JOM, 2017, 69: 1801−1805.

[19] JIANG Tao, WANG Shuai, GUO Yu-feng, CHEN Feng, ZHENG Fu-qiang. Effects of basicity and MgO in slag on the behaviors of smelting vanadium titanomagnetite in the direct reduction-electric furnace process [J]. Metals, 2016, 6: 107−122.

[20] WANG Shuai, GUO Yu-feng, JIANG Tao, YANG Lu, CHEN Feng, ZHENG Fu-qiang, XIE Xiao-lin, TANG Min-jun. Reduction behaviors of iron, vanadium and titanium oxides in smelting of vanadium titanomagnetite metallized pellets [J]. JOM, 2017, 69: 1646−1653.

[21] ZHANG L, ZHANG L N, YANG M Y, LOU T P, SUI Z T, JANG J S. Effect of perovskite phase precipitation on viscosity of Ti-bearing blast furnace slag under the dynamic oxidation condition [J]. Journal of Non-crystalline Solids, 2006, 352: 123−129.

[22] WEARING E. An intergrown perovskite-wollastonite phase in some ferrous blast-furnace slags [J]. Journal of Materials Science, 1983, 18: 1629−1637.

[23] LI Yu-hai, LOU Tai-ping, XIA Yu-hu, SUI Zhi-tong. Kinetics of non-isothermal precipitation process of the perovskite phase in

$CaO-TiO_2-SiO_2-Al_2O_3-MgO$ system [J]. Journal of Materials Science, 2000, 35: 5635−5637.

[24] ZHAO B J, JAK E, HAYES P C. Fundamental studies in ironmaking slags to lower operating temperatures and to recover titania from slag [J]. Journal of Iron and Steel Research International, 2009, 16: 1172−1178.

[25] SHANKAR A, GORNERUP M, LAHIRIL A K, SEETHARAMAN S. Experimental investigation of the viscosities in $CaO-SiO_2-MgO-Al_2O_3$ and $CaO-SiO_2-MgO-Al_2O_3-TiO_2$ slags [J]. Metallurgical and Materials Transactions B, 2007, 38: 911−915.

[26] BALE C W, BÉLISLE E, CHARTRAND P, DECTEROV S A, ERIKSSON G, GHERIBI A E, HACK K, JUNG I H, KANG Y B, MELANÇON J, PELTON A D. FactSage thermochemical software and databases, 2010−2016 [J]. Calphad, 2016, 54: 35−53.

[27] HUANG Xi-hu. Iron and steel metallurgy principle [M]. 4th ed. Beijing: Metallurgical Industry Press, 2013. (in Chinese)

[28] LI Wei, FU Gui-qin, CHU Man-sheng, ZHU Miao-yong. Gas-based direct reduction of Hongge vanadium titanomagnetite-oxidized pellet and melting separation of the reduced pellet [J]. Steel Research International, 2017, 88: 1−10.

[29] DU He-gui. The principle of smelting the vanadium titanomagnetite ore in the blast furnace [M]. Beijing: Science Press, 1996. (in Chinese)

[30] WANG Ming-yu, WANG Xue-wen, HE Yue-hui, LOU Tai-ping, SUI Zhi-tong. Isothermal precipitation and growth process of perovskite phase in oxidized titanium bearing slag [J]. Transactions of Nonferrous Metals Society of China, 2008, 18: 459−462.

电炉法冶炼钒钛磁铁矿金属化球团的适宜钛渣组成

王 帅，郭宇峰，姜 涛，陈 凤，郑富强，唐敏俊，杨凌志，邱冠周

中南大学 资源加工与生物工程学院，长沙 410083

摘 要：对适宜于预还原电炉法冶炼钒钛磁铁矿的较高品位钛渣的组成进行研究。根据热力学分析结果和相图中的低熔点区域，建议的高品位直接还原电炉钛渣组成为约 50% TiO_2，8%~12% MgO 和 13% Al_2O_3 (质量分数)，二元碱度范围为 0.8~1.2。电炉及感应炉验证实验表明，在所推荐的钛渣组成下，可实现渣铁的成功分离。所得的含钒铁水含有 0.681% V 和 0.267% Ti (质量分数)；所得钛渣以黑钛石($MgTi_2O_5$)为主要物相，其 TiO_2 品位为 52.21%(质量分数)。所得钛渣可满足后续采用酸法浸出回收钛的要求。

关键词：钒钛磁铁矿；电炉；碱度；氧化镁；黑钛石($MgTi_2O_5$)；钛渣组成

(Edited by Bing YANG)